SUPPLEMENTARY INFORMATION
https://doi.org/10.1038/s42255-018-0001-z

nature metabolism

In the format provided by the authors and unedited.

GIP regulates inflammation and body weight by restraining myeloid-cell-derived S100A8/A9

Fernanda Dana Mantelmacher[1,7], Isabel Zvibel[1,7], Keren Cohen[1], Alona Epshtein[1], Metsada Pasmanik-Chor[2], Thomas Vogl[3], Yael Kuperman[4], Shai Weiss[1], Daniel J. Drucker[5], Chen Varol[1,6]* and Sigal Fishman[1]*

[1]The Research Center for Digestive Tract and Liver Diseases, Tel-Aviv Sourasky Medical Center and the Sackler School of Medicine, Tel-Aviv University, Tel-Aviv, Israel. [2]Bioinformatics Unit, Faculty of Life Science, Tel Aviv University, Tel-Aviv, Israel. [3]Institute of Immunology, University of Münster, Münster, Germany. [4]Department of Veterinary Resources, Weizmann Institute of Science, Rehovot, Israel. [5]The Lunenfeld-Tanenbaum Research Institute, Mount Sinai Hospital, University of Toronto, Toronto, Ontario, Canada. [6]Department of Clinical Microbiology and Immunology, Sackler School of Medicine, Tel-Aviv University, Tel-Aviv, Israel. [7]These authors contributed equally: Fernanda Dana Mantelmacher, Isabel Zvibel. *e-mail: chenv@tlvmc.gov.il; sigalf@tlvmc.gov.il

Supplementary information

Supplementary figures

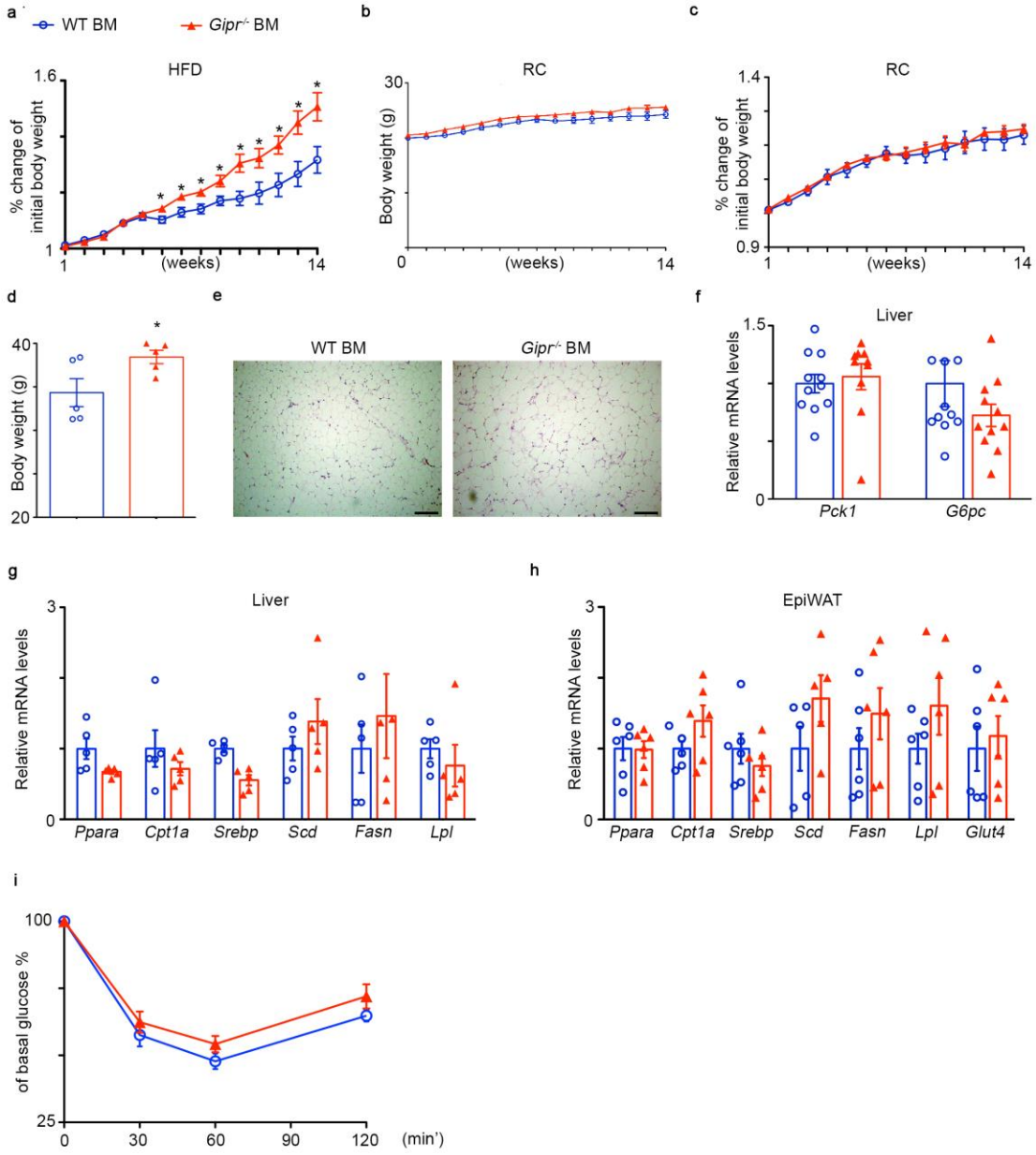

Supplementary Figure 1: Metabolic parameters in WT and *Gipr*$^{-/-}$ BM mice.

Mice were reconstituted with WT BM (blue open circles) or *Gipr*$^{-/-}$ BM (red triangles) for 6 weeks and then fed with RC or HFD for 14 weeks or 18 weeks. (**a**) Percentage of weight gain (%) from initial weight in WT BM (blue open circles) or *Gipr*$^{-/-}$ BM fed HFD for 14 weeks (n=10, time point week 6-14 p=0.013, P=0.014, P=0.014, P=0.015,

P=0.01, P=0.04, P=0.03, P=0.016, P=0.022) (**b**) Body weight gain of mice under RC (g) (n=5 each group). (**c**) Body weight gain under RC (%) (n=5 each group) (**d**) Final body weight of mice reconstituted with WT BM or *Gipr*$^{-/-}$ BM after 18 weeks HFD (g) (n=5, P=0.051). (**e**) Representative H&E sections of ingWAT of mice reconstituted with WT BM or *Gipr*$^{-/-}$ BM Original magnification x10. Bars, 200 μm. (**f**) Hepatic expression of gluconeogenesis genes after 14 weeks HFD was determined by qRT-PCR and normalized to *Rplp0* (n=11). (**g**) Hepatic expression of lipogenesis and β-oxidation genes after 14 weeks HFD was determined by qRT-PCR and normalized to *Rplp0* (n=5 each group). (**h**) Expression of metabolic genes after 14 weeks HFD was assessed in epiWAT and normalized to *Rplp0* (n=6 each group). (i) ITT showing % of basal glucose in WT BM and *Gipr*$^{-/-}$ BM mice from Fig.1h (WT BM mice n=6, *Gipr-/-* BM mice n=5). Data were analyzed by unpaired, two-tailed *t*-test, comparing each time between WT BM and *Gipr*$^{-/-}$ BM mice, and are presented as mean ± SEM. Data in a-b are from single experiments and in d-f from two separate experiments.

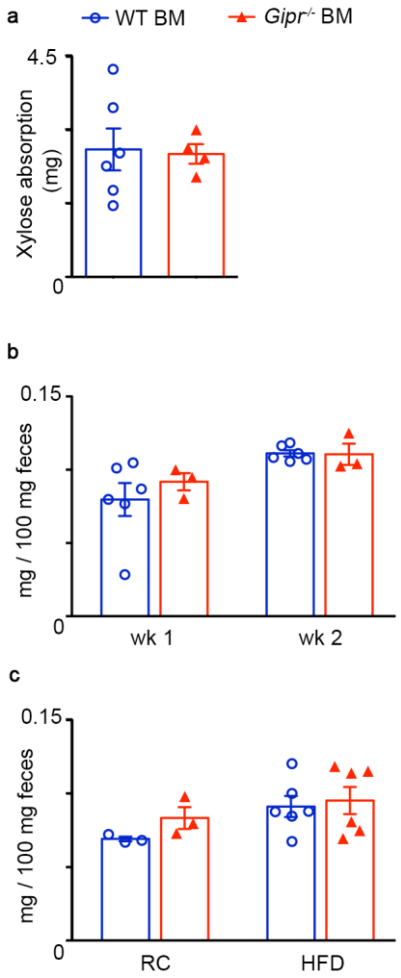

Supplementary Figure 2: *Gipr*$^{-/-}$ BM mice do not have impaired intestinal absorption either during the bone marrow reconstitution phase or during the HFD feeding period. Mice were reconstituted with WT BM (blue open circles) or *Gipr*$^{-/-}$ BM (red triangles) for 6 weeks and then fed RC or HFD. (**a**) Six weeks after BM reconstitution and 2 weeks following RC feeding, a xylose absorption test was performed in the chimeric mice. Graph shows similar absorption in both groups (n=6 for WT BM mice, n=4 for *Gipr*$^{-/-}$ BM mice). (**b**) Fat content in feces was measured under RC at one week (n=5 for WT BM mice, n=3 for Gipr-/- BM mice) and two weeks (n=6 for WT BM mice, n=3 for *Gipr*$^{-/-}$ BM mice) during the reconstitution period, as well as after five weeks of HFD (n=3 each group) or RC (n=6 each group)

(**c**). Data were analyzed by unpaired, two-tailed *t*-test, comparing each time between WT BM and *Gipr*$^{-/-}$ BM mice, and are presented as mean ± SEM.

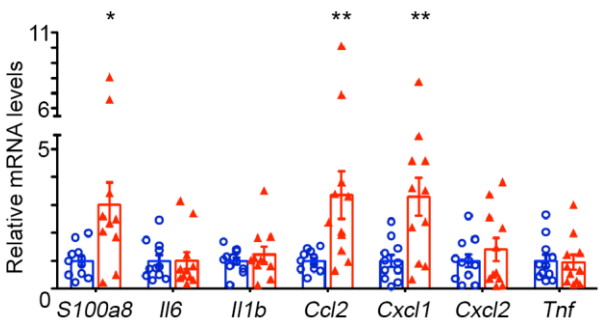

Supplementary Figure 3: Hepatic expression of inflammatory mediators. The expression of inflammatory cytokines and chemokines genes after 14 weeks of HFD was determined by qRT-PCR and normalized to *Rplp0* (n=11 each group, for *S100a8* p=0.016, for *Ccl2* p=0.012, for *Cxcl1* p=0.004). Data were analyzed by unpaired, two-tailed *t*-test, comparing between WT BM and *Gipr*$^{-/-}$ BM mice and the results are presented as mean ± SEM.

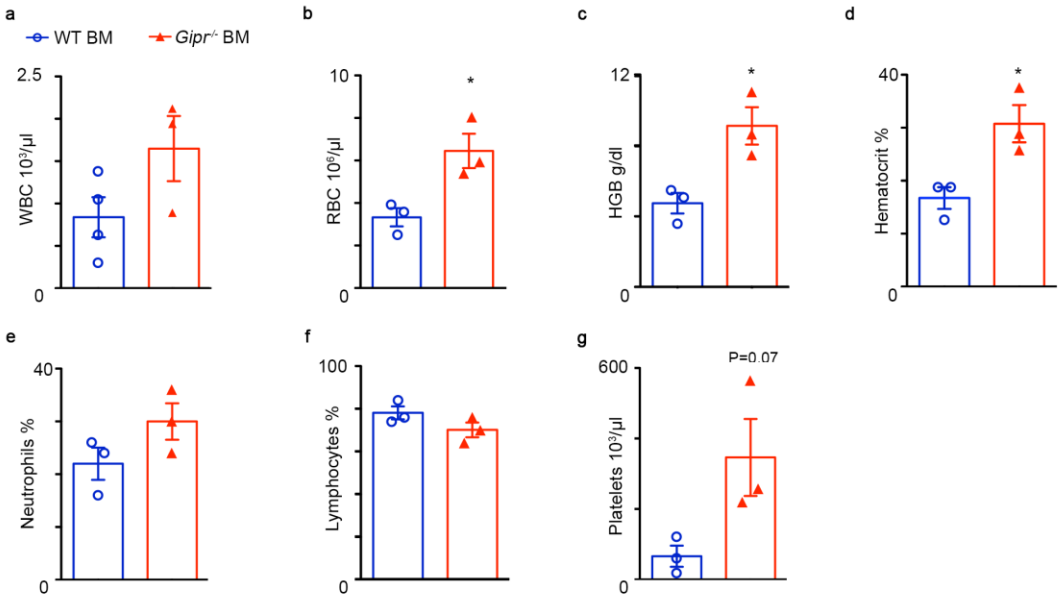

Supplementary Figure 4: Blood count of WT BM versus *Gipr*$^{-/-}$ BM mice on HFD. Mice were reconstituted with WT BM (blue open circles, n=4 mice) or *Gipr*$^{-/-}$ BM (red triangles, n=3 mice) for 6 weeks and then fed HFD for 14 weeks. (a) White blood cell (WBC) count (ul). (b) Red blood cell (RBC) count (ul) (p=0.027). (c) Hemoglobin (HGB) count (dl) (p=0.022). (d) Hematocrit (p=0.026) (e) % Neutrophils and (f) Lymphocytes % from serum. (g) Platelets (p=0.068) (ul). Data were analyzed by unpaired, two-tailed *t*-test, comparing between WT BM and *Gipr*$^{-/-}$ BM mice and the results are presented as mean ± SEM. Data are from a single experiment.

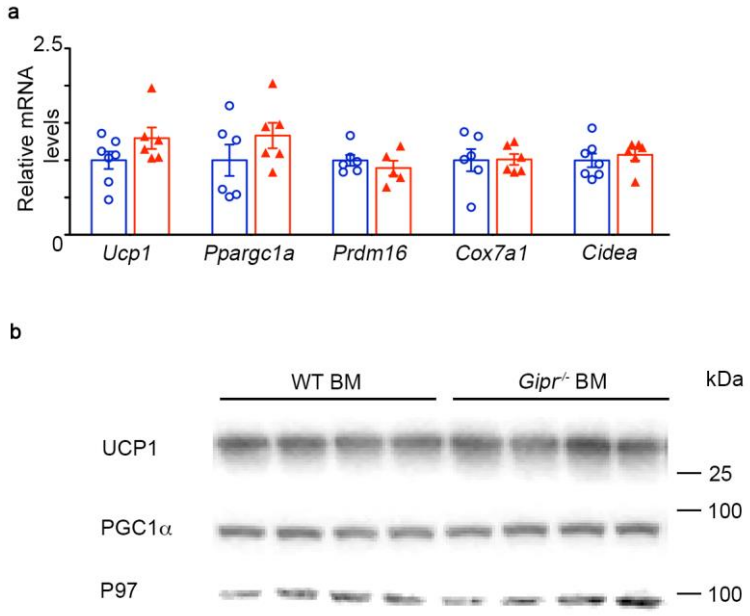

Supplementary Figure 5: Molecular markers of thermogenesis in brown adipose tissue (BAT).

Mice were reconstituted with WT BM (blue open circles) or *Gipr*$^{-/-}$ BM (red triangles) for 6 weeks and then fed HFD for 14 weeks. (**a**) Expression of BAT thermogenesis genes was assessed by qRT-PCR and normalized to *Rplp0* (WT BM n=7, *Gipr*$^{-/-}$ BM n=6). (**b**) Representative immunoblots of thermogenesis proteins UCP1 and PGC1α in BAT demonstrating similar expression of the proteins in the two groups of mice. P97 was used as control (n=4 each group). Data were analyzed by unpaired, two-tailed *t*-test, comparing between WT BM and *Gipr*$^{-/-}$ BM mice, and are presented as mean ± SEM. Data represent two independent experiments.

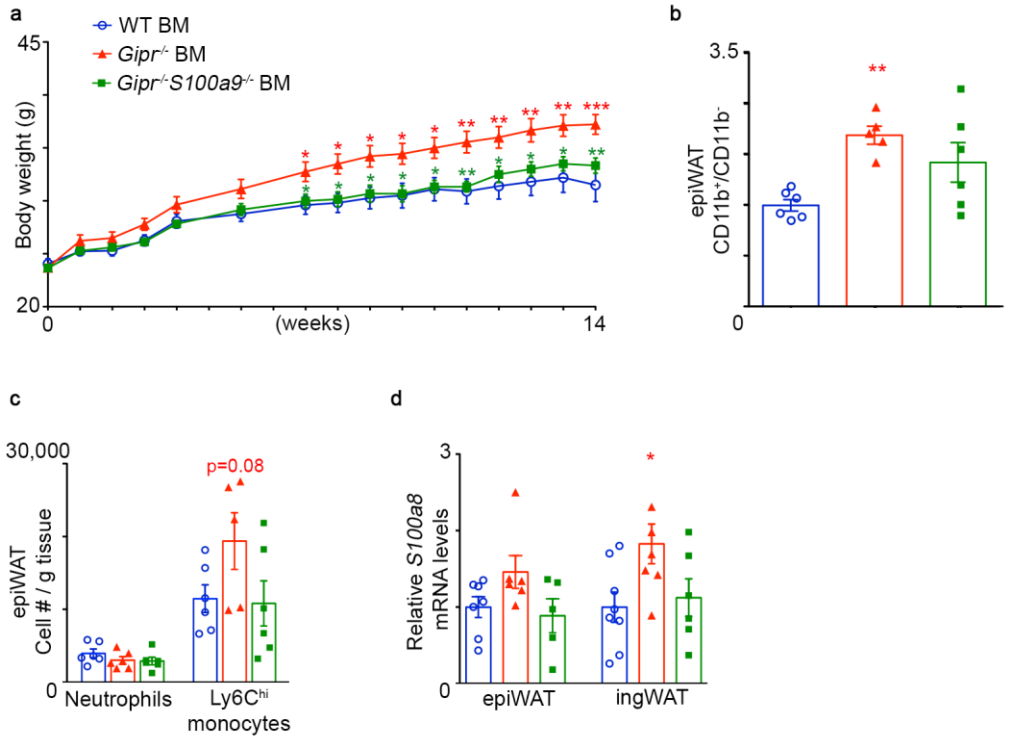

Supplementary Figure 6: Double deletion of GIPR and S100A8/A9 from immune cells reverses the metabolic and myelopoiesis phenotypes displayed by *Gipr*$^{-/-}$ BM mice also at 18 weeks of HFD. Mice were reconstituted with WT BM (blue open circles), *Gipr*$^{-/-}$ BM (red triangles) and *Gipr*$^{-/-}$*/S100a9*$^{-/-}$ BM (green squares) for 6 weeks and then fed with HFD for 18 weeks. (**a**) Weekly measurements of body weight (n=6). (**b**) Graphs showing as indication for myelopoiesis the ratio of CD11b^{+} phagocytes vs. CD11b^{-} lymphocytes in the epiWAT (n=6). (**c**) Bar graphs showing numbers of neutrophils and Ly6C^{hi} monocytes normalized per tissue mass in the epiWAT (n=6). (**d**) qRT-PCR assessment of *S100a8* expression normalized to *Rplp0* in the ingWAT and epiWAT (WT BM mice n=10, *Gipr*$^{-/-}$ BM mice n=10, *Gipr*$^{-/-}$*/S100a9*$^{-/-}$ BM mice n=8). Data were analyzed by one way ANOVA with Bonferroni and are presented as mean ± SEM with significance: *p<0.05 **p<0.01 ***p<0.001. Red stars represent significance of *Gipr*$^{-/-}$ BM group vs. WT BM. Green stars

represent significance of *Gipr*$^{-/-}$/*S100a9*$^{-/-}$ BM vs. *Gipr*$^{-/-}$ BM. Data are from a single experiment.

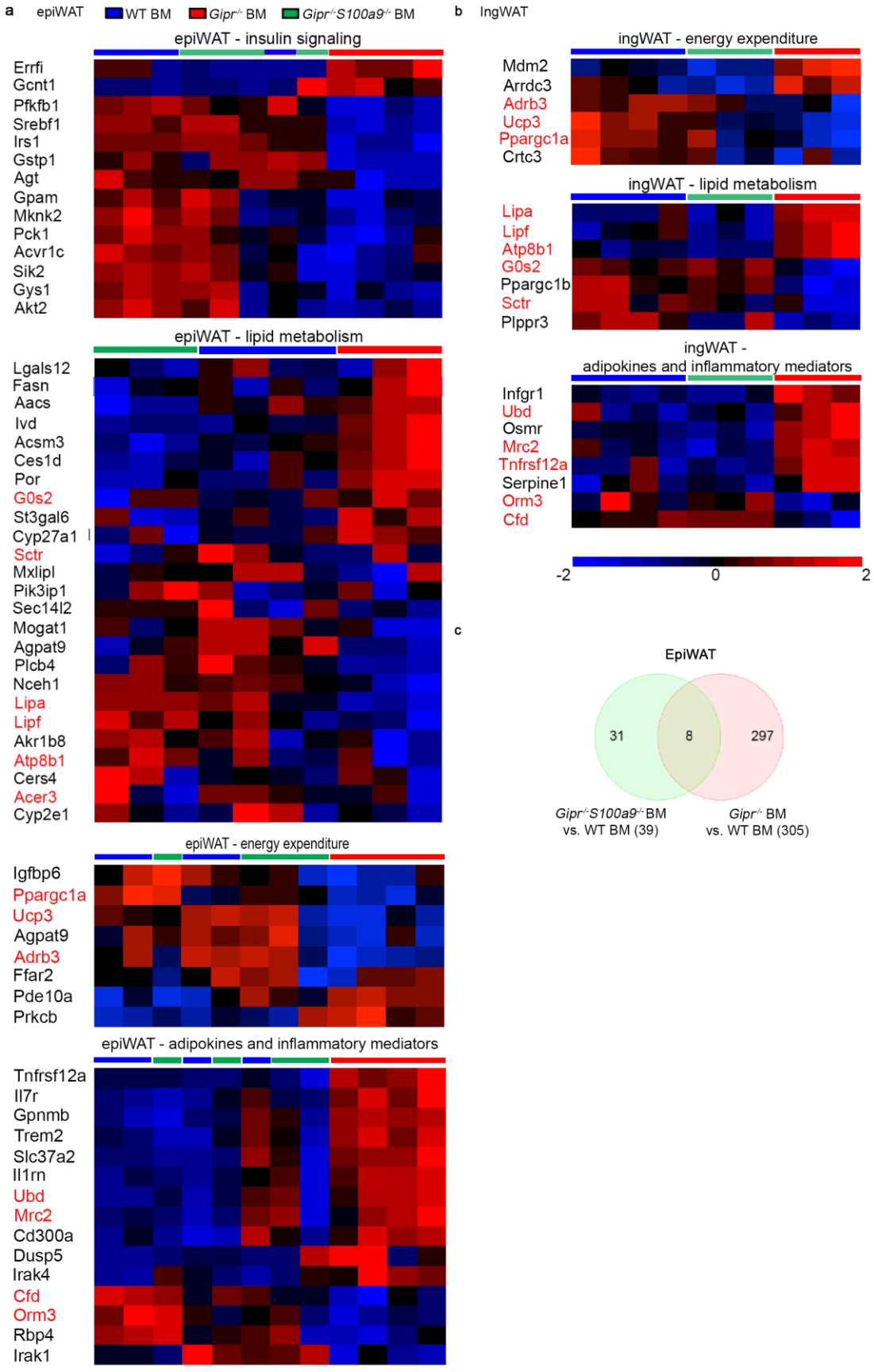

Supplementary Figure 7: Double deletion of GIPR and S100A8/A9 from immune

cells reverses the gene expression alterations observed in epiWAT and ingWAT of *Gipr*$^{-/-}$ BM mice.

Mice were reconstituted with WT BM (blue), *Gipr*$^{-/-}$ BM (red) and *Gipr*$^{-/-}$*/S100a9*$^{-/-}$ BM (green) for 6 weeks and then fed with HFD for 14 weeks. Subsequently, mRNA was extracted from epiWAT and ingWAT and subjected to Affymetrix gene array. Differentially expressed genes were obtained using a cut off of at least 2-fold change (p value <0.05). Venn diagram showing the distribution of 336 genes (epiWAT) and of 1455 genes with above 2-fold expression difference in the comparison between *Gipr*$^{-/-}$*S100a9*$^{-/-}$ BM vs. WT BM and *Gipr*$^{-/-}$ BM vs. WT BM. (**a**) Heatmaps visualizing the hierarchical clustering of differentially expressed genes (Fold-change ≥2, p<0.05, ANOVA) that are associated with pathways in epiWAT: insulin signaling, lipid metabolism, energy expenditure and adipokines and inflammatory mediators (n≥3). (**b**) Heatmaps visualizing the hierarchical clustering of differentially expressed genes (Fold-change ≥2, p<0.05, ANOVA) that are associated with pathways in ingWAT: energy expenditure, lipid metabolism and adipokines and inflammatory mediators (n≥3). Genes that are altered in both epiWAT and ingWAT are marked with red color. Data are from a single experiment. (**c**) Venn diagram showing the distribution of 336 genes with above 2-fold expression difference in the comparison between epiWATs of *Gipr*$^{-/-}$*S100a9*$^{-/-}$ BM vs. WT BM and *Gipr*$^{-/-}$ BM vs. WT BM.

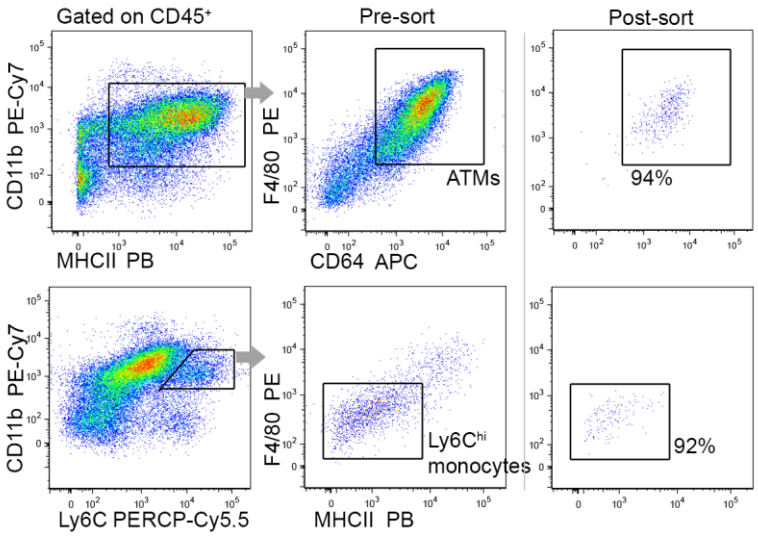

Supplementary Figure 8: Gating strategy used to sort Ly6c^{hi} monocytes and ATM from epiWAT of mice fed HFD for 14 weeks. Left panel, flow cytometry images showing the gating strategy used for the sorting of Ly6c^{hi} monocytes (n=15 mice) and ATMs (n=5, three repetitions) from epiWAT of WT mice fed with HFD for 14 weeks. Right panel, flow cytometry images showing sorting purity for each of the indicated populations.

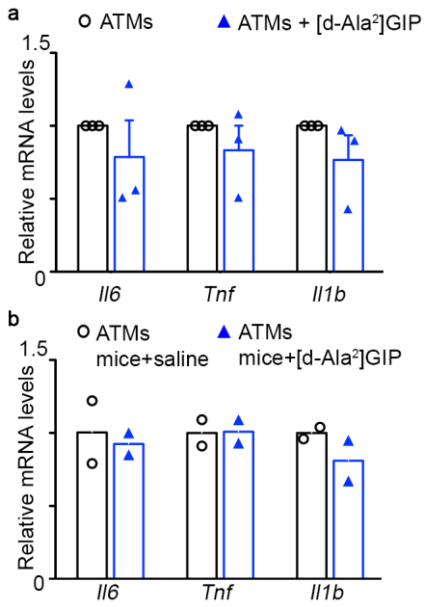

Supplementary Figure 9: GIP treatment does not affect the gene expression of other inflammatory cytokines in sorted ATMs. Expression of inflammatory cytokines analyzed by qRT-PCR and normalized to *Tbp* in (**a**) ATMs sorted from epiWAT of WT mice after 14 weeks of HFD and following *ex vivo* 24 h treatment with 100nM d[Ala2]-GIP or vehicle ($PBS^{-/-}$). Cytokine expression is presented as fold induction versus untreated controls. (n= 3, each repeat represents a pool of 5 mice). (**b**) Expression of inflammatory cytokines analyzed by qRT-PCR and normalized to *Tbp* in sorted ATMs from epiWAT of WT mice after 14 weeks of HFD and daily i.p injections of d[Ala2]-GIP (0.12μg/g body weight) or vehicle ($PBS^{-/-}$) during the last eight weeks (n= 2, each repeat represents a pool of 5 mice).

Figure 1m

pAKT

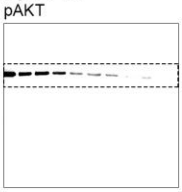

AKT

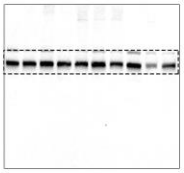

Figure 1n

pAKT

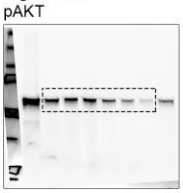

AKT

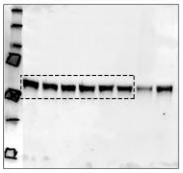

Figure 2b

S100A8

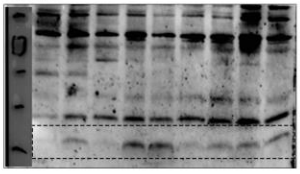

P97

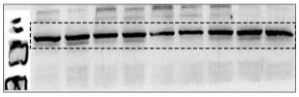

Figure 3e

UCP1

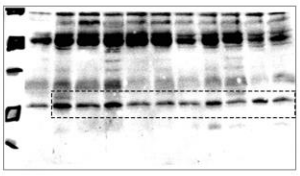

P97

Figure 3g

PGC1α

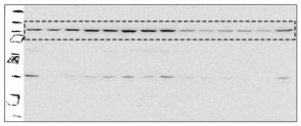

UCP1

P97

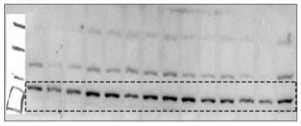

P97

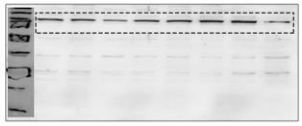

Figure 6n

PGC1

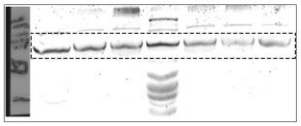

P97

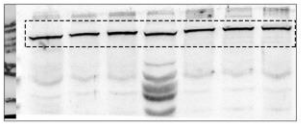

Supplementary Figure 10: Original Western blots

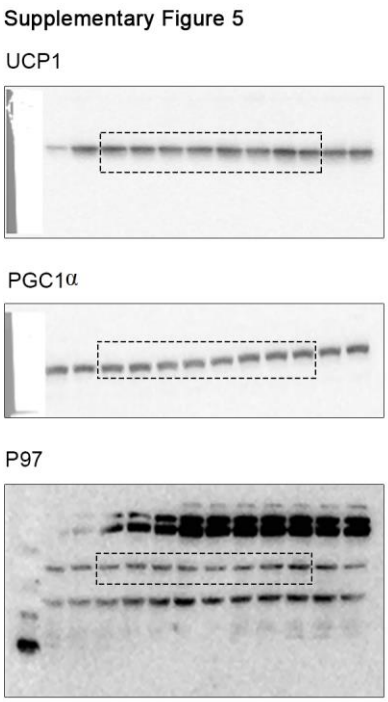

Supplementary Figure 11: Original Western blots of supplementary Figure 5.

Supplementary Table 1: Antibodies used for flow cytometry

Antibody	**Source**	**Catalog number**
APC anti-mouse CD64 (FcγRI) Antibody	Biolegend	Cat# 139306
APC/Cy7 anti-mouse CD45 Antibody	Biolegend	Cat# 103116
Brilliant Violet421 anti-mouse Ly6G Antibody	Biolegend	Cat# 127628
Pacific Blue anti-mouse I-A/I-E Antibody	Biolegend	Cat# 107620
PerCP/Cy5.5 anti-mouse Ly6C Antibody	Biolegend	Cat# 128012
PE anti-mouse CD115 (CSF-1R) Antibody	Biolegend	Cat# 135506
PE/Cy7 anti-mouse/human CD11b Antibody	Biolegend	Cat# 101216
PE rat anti-mouse F4/80 Antibody	Bio-Rad	Cat# MCA497RT
Alexa 647 anti- rabbit antibody	Jackson	Cat#711605152

Supplementary Table 2: Sequences of murine oligonucleotide primers for qRT-PCR

Gene	**Left primer**	**Right primer**
Sterol regulatory element-binding protein-1 (*Srebp)*	GCGCTACCGGTCTTCTATCA	TGTGCACTTCGTAGGGTCAG
Fatty acid synthase (*Fasn*)	ATTGTCGCTCTGAGGCTGTT	GCTGGCTGATACAGAGAGCA
Stearoyl-Coenzyme A desaturase-1 (*Scd*)	TGCGATACACTCTGGTGCTC	TAGTCGAAGGGGAAGGTGTG
Lipoprotein lipase (*Lpl*)	GGGCTCTGCCTGAGTTGTAG	CCACCTCAGTCCCAGAAAA
Peroxisome proliferator	ATGCCAGTACTGCCG	TTGCCCAGAGATTTG

activated receptor alpha (*Ppara*)	TTTTC	AGGTC
Carnitine palmitoyltransferase (*Cpt1a*)	CATGTCAAGCCAGACGAAGA	CTTTCGACCCGAGAAGACCT
Glucose transporter type 4 (*Glut4*)	AGCGAGTGACTGGAACACTG	AGAGCCCAGAGCGTAGTGAG
Calcium-binding protein A8 (*S100a8*)	GGAAATCACCATGCCCTCTA	TGGCTGTCTTTGTGAGATGC
Calcium-binding protein A9 (*S100a9*)	GAAGGAAGGACACCCTGACA	TCAACTTTGCCATCAGCATC
Interleukin 6 (*Il6*)	CCGGAGAGGAGACTTCACAG	TTCTGCAAGTGCATCATCGT
Interleukin 1β (*Il1b*)	GACCTTCCAGGATGAGGACA	AGCTCATATGGGTCCGACAG
Chemokine (C-C motif) ligand 2 (*Ccl2*)	AGGTCCCTGTCATGCTTCTG	GCTGCTGGTGATCCTCTTGT
Chemokine (C-X-C motif) ligand 1 (*Cxcl1*)	CTTGAAGGTGTTGCCCTCAG	TCTGAACCAAGGGAGCTTCA
Chemokine (C-X-C motif) ligand 2 (*Cxcl2*)	AGTGAACTGCGCTGTCAATG	TTCAGGGTCAAGGCAAACTT
Thermogenin Uncoupling protein 1 (*Ucp1*)	CTTCTCAGCCGGAGTTTCAG	GGCAATCCTTCTGTTTTTGC
Peroxisome proliferator-activated receptor gamma coactivator 1-alpha	AATGCAGCGGTCTTAGCACT	GTGTGAGGAGGGTCATCGTT

(*Ppargc1a*)		
PR domain containing 16 (*Prdm16*)	GATCTTCCCCAGATCTGCAA	ACGGCTTCTCTTTGTTGTGG
Cytochrome c oxidase polypeptide 7A1 (*Cox7a1*)	AAAACCGTGTGGCAGAGAAG	CAGCGTCATGGTCAGTCTGT
Cell death activator CIDE-A (*Cidea*)	TGGAAAAGGGACAGAAATGG	TCTCGTACATCGTGGCTTTG
Glucose-dependent insulinotropic polypeptide receptor (*Gipr*)	GTGTCTTGCCCCTGGTATCT	AGCCCCATTCTTCTCTGGAT
CD137 Tumor necrosis factor receptor superfamily, member 9 (*Tnfrsf9*)	GCCCTCCAAGTACCTTCTCC	GCCTGCAGTCCTTTTCACAT
β adrenergic receptor 3 (*Adrb3*)	ACAGGAATGCCACTCCAATC	TTAGCCACAACGAACACTCG
Thermogenin Uncoupling protein 3 (*Ucp3*)	ATGAGTTTTGCCTCCATTCG	GGCGTATCATGGCTTGAAAT
Transcription factor A, mitochondrial *(Tfam)*	CCGAAGTGTTTTTCCAGCAT	GGCTGCAATTTTCCTAACCA
Nuclear respiratory factor 1 *(Nrf1)*	AAAGCTGCAAGCCTATCTGG	GGTGGCCTGAGTTTGTGTTT
Cytochrome oxidase subunit 4i1*(Cox4i1)*	ACCGCATCCAGTTTAACGAG	CCCAGTCACGATCGAAAGTA

T-box1 *(Tbx*)	CGACAAGCTGAAACTGACCA	GTGACTGCAGTGAAGCGTGT
Acidic ribosomal protein P0*(Rplp0*)	CAACCCAGCTCTGGAGAAAC	GTTCTGAGCTGGCACAGTGA
TATA box binding protein (*Tbp)*	CCCCACAACTCTTCCATTCT	CAGCCAAGATTCACGGTAGA